

## REMOTE OBJECTIVE SPECKLE DISPLACEMENT SENSITIVITY

T. D. Dudderar,\* J. A. Gilbert,<sup>†</sup> J. H. Bennewitz,\* E. J. Van Rossum<sup>‡</sup>

### ABSTRACT

The coarse objective speckle pattern which is reflected from a suitably illuminated moving surface can readily be sampled by an optical fiber bundle and input through it to a remote photoelectronic/computer system for analysis and interpretation. In correctly interpreting such data it is very important to relate the measured speckle motion to the actual surface motion accurately. If the beam of coherent illumination responsible for the formation of the objective speckle is either converging or diverging, the resulting objective speckle field will appear to rotate about the symmetric image of the apparent point source of the illumination. Consequently, by properly choosing the sampling distance and illuminating beam divergence (or convergence), the sensitivity may be made much larger (or smaller) than one, as desired.

### Introduction

Earlier studies by the authors<sup>(1-5)</sup> have demonstrated the application of fiber optics and photoelectronic digitization/computer correlation techniques to speckle metrology. Figure 1 shows a schematic diagram of the typical arrangement used in most of these studies. Here a single mode fiber (SMF) is used to illuminate a small area on a remote test surface. Illumination of a small area of any diffusely reflecting surface<sup>+</sup> gives rise to a three-dimensional field of random speckles associated with constructive and destructive interference of coherent light. A normal cross-section of this objective field, as it falls on the input end of the multimode image bundle (MMB) positioned to sample the remote speckle field at Z, provides a pattern of light and dark regions uniquely associated with the illuminated spot on the surface. If the surface spot moves, this objective speckle pattern moves as well. Out-of-plane movements will be manifest in changes in the transverse size statistics of the speckles while all in-plane movements give rise to translations of the speckle pattern itself. Successive speckle patterns associated with various positions of a surface subjected to in-plane motion may thus be digitized, stored and subsequently analyzed by the computer to determine this motion at any illuminated points on the test surface as desired.

Of course, accurate interpretation of in-plane displacement depends on knowledge of the relationship

between objective speckle movement as it appears (and is digitized) on the monitor screen, and the actual in-plane displacement of the remote test surface. The system magnification,  $S_e$ , (from the output end of the MMB through an imaging lens into the vidicon camera tube and onto the monitor) depends on the system itself and may readily be calibrated for a given set-up by laterally displacing either end of the MMB a known amount. (The MMB itself has an end-to-end magnification of unity, so it doesn't matter which end is moved.) However, the relationship between a) the movement of the speckle as sampled by the input to the MMB at Z and b) the transverse movement of the test surface itself is not unique. In fact, it depends on various parameters of the fiber-optic configuration used to generate and sample the objective speckle field, as well as the movement of the surface itself.

In the simplest case, if the illumination is collimated (such as might be obtained by either using an unspread beam directly from a laser, or by collimating the output from the SMF with a separate lens or lens system) the speckle field translates with the surface. Consequently, a unit displacement of the test surface results in an identical unit displacement of the speckle field input to the MMB, regardless of the angle of illumination or where<sup>•</sup> it is sampled by the MMB.

\* AT&T Bell Laboratories, Murray Hill, NJ 07974

<sup>†</sup> Associate Professor of Engineering Mechanics, Department of Civil Engineering, University of Wisconsin-Milwaukee, Milwaukee, WI 53201.

<sup>‡</sup> Graduate student in Engineering Mechanics, Department of Civil Engineering, University of Wisconsin-Milwaukee, Milwaukee, WI 53201

<sup>+</sup> A diffusely reflecting surface is a surface whose roughness dimension is large in comparison to the wavelength of light.

<sup>•</sup> If the sampling plane itself (the input face of the MMB) is inclined at an angle  $\alpha$  from the normal to the test surface it will resolve the  $\cos \alpha$  component of the objective speckle field motion at that point, be it translating, rotating or whatever.



However, it has been observed<sup>(4)</sup> that whenever an un lensed SMF is used to provide an illumination beam, the overall system sensitivity appears to change as a function of both  $Z$  and either the illuminated spot size or the SMF-to-surface distance, or both. Since the system configuration was essentially unchanged throughout most of these studies, these changes had to be the result of induced "rotations" of the objective speckle field. In many instances the speckle pattern sampled by the MMB translated much faster than did the point on the surface being illuminated, which represented a significant unaccounted for increase in sensitivity. Moreover, with the addition of lenses to provide beams of converging illumination it was observed that, depending on where the sampling was accomplished, the speckle pattern might be seen to a) move rapidly in the opposite direction to the surface, b) not move at all (just "boil" while the surface moves), or c) move very slowly in the same direction as the surface motion. Earlier,<sup>(4)</sup> efforts to interpret this behavior in terms of the effective numerical aperture,  $NA$ , of the illumination beam, the diameter,  $D$ , of the illuminated spot on the test surface and the MMB sampling distance,  $Z$ , were relatively unsuccessful owing primarily to insufficient accuracy in determining  $D$  and  $NA$  using lensed SMF illumination. In the present study, the objective speckle motion has been examined using un lensed SMF's of two independently determined  $NA$ 's, and considering only the two parameters  $Z$  and the wavefront radius of curvature,  $\rho$ ,<sup>□</sup> rather than  $Z$ ,  $NA$ , and  $D$ .

### Experiment

Two series of tests were run using the configuration shown in Figure 1 with the test surface mounted on a micrometer driven translation stage. In the first series of tests an SMF of  $NA = 0.105$  was positioned at five different illuminating distances from the test surface (1.20 mm, 1.60 mm, 4.40 mm, 15.90 mm and 25.40 mm as measured to an accuracy of  $\pm 0.5$  mm). For a fixed sampling distance of  $Z = 101.6$  mm, an overall sensitivity,  $S$ , in columns/mm was determined for each (illumination distance) by carefully translating the test surface laterally far enough to move the speckle field on the monitor 100 digitized raster lines, noting the required surface translation,  $\Delta X$ , and converting. Since the core of the SMF is only around  $6-7 \mu\text{m}$  in diameter, the illumination distance was taken to be a reasonable estimate of the radius of curvature,  $\rho$ , of the illuminating wave front as it strikes the surface. Table I gives the overall sensitivity,  $S$ , versus  $\rho$  for these tests, along with the results for a single test run with the SMF replaced by an unspread beam direct from the laser such that  $\rho = \infty$  (collimated illumination). In these tests the system magnification,  $S_c$ , was field calibrated to give 58.6 raster columns of

movement on the monitor for each millimeter of lateral translation at the MMB. Subsequently, a second series of tests were run using an SMF of  $NA = 0.119$  at eight different distances (1.5 mm, 3.1 mm, 6.1 mm, 12.2 mm, 24.4 mm, 48.8 mm, 76.2 mm and 101.6 mm, again as measured to an accuracy of  $\pm 0.5$  mm) and four more sampling distances. As listed in Table II, these ranged from 50.8 mm up to 812.8 mm, the greatest sampling distance for which there was sufficient intensity to generate worthwhile speckle patterns at all  $\rho$ 's. Since the system had been rebuilt and refocused it was recalibrated to yield a system magnification,  $S_c$ , of 53.93 col/mm.

### Analysis and Discussion

In each case the total sensitivity,  $S$ , defining the raster columns of shift per millimeter of lateral surface displacement, was converted to objective speckle magnification,  $M$ , in millimeters of speckle movement per millimeter of lateral surface displacement, by dividing by the appropriate system sensitivity,  $S_c$ . The resulting values of  $M$  are given in Tables I and II and plotted against  $\rho$  in Figure 2. In these data the objective speckle magnification ranges from near unity at  $\rho = \infty$  to almost 600 at  $\rho = 1.5$  mm and  $Z = 812.8$  mm. The data shown in Figure 2 as a log-log plot form an array of almost linear, equally spaced curves which fan out slightly as  $\rho \rightarrow 0$  and  $M$  increases. Moreover, as  $\rho \rightarrow \infty$ , where it would be expected that  $M \rightarrow 1$  and the curves would flatten, some decrease in slope appears at smaller  $Z$ 's.

Figure 3 provides a simplified geometrical description of the speckle field movement appropriate to model this data. As the surface moves laterally a distance  $\Delta X$ , the illumination reflected to the sample plane at  $Z$  moves a distance  $\Delta X'$ . It is as if the speckle field rotates about  $P'$ , a virtual image of the point source of illumination at  $P$ . The location of  $P'$  is shown in the figure by the dotted lines converging at a distance  $\rho$  behind the test surface. Defining the objective speckle magnification,  $M$ , as  $\Delta X'/\Delta X$ , by geometry we may compute

$$M = (\rho + Z)/\rho \quad (1)$$

This analysis assumes that the rays of illumination are reflected at their angles of incidence, which is somewhat at odds with the fact that the surface must be diffusely reflecting so as to form speckle. Nevertheless, it represents a reasonable first order description of the geometry of objective speckle field movement with noncollimated illumination, regardless of the actual statistics of the interference contributing to the speckle formation itself. As empirical evidence of this, Figure 4 shows a log-log plot of  $(\rho + Z)/\rho$  versus  $M$ . Here it can clearly be seen that at smaller  $M$ 's the data groups closely along a single straight line of slope  $\sim 1$ , although there is some spread in values as  $M$  becomes large. However,

□ As suggested by K. A. Stetson.



considering the uncertainty in determining  $\rho$ , together with the limited resolution (0.0025 mm) of the micrometers used to translate the test surface, this scatter at large  $M$ 's (small  $\rho$ 's) is quite moderate and probably does not represent any significant departure from the trend established at smaller  $M$ 's. Consequently, for all data  $M$  may reasonably be taken to be proportional to  $(\rho + Z)/\rho$  and that the simple relation given by equation (1) is valid for at least a first order estimate of  $M$ .

Furthermore, equation (1) also indicates that if  $\rho$  is negative, denoting a converging rather than diverging illumination beam, the sign of  $M$  will change as  $Z$  varies from less to more than  $|\rho|$ . In this case the image of the point source lies in front of the test surface at a distance  $|\rho|$ . Consequently, different regions of the three-dimensional objective speckle field which forms in front of the test surface rotate with or against the surface motion as it pivots. At  $Z$  less than  $|\rho|$  the magnification,  $M$ , is positive and the speckle movement will be in the same direction as the surface movement but reduced,  $M < 1$ . At  $Z = |\rho|$  the magnification,  $M$ , becomes zero and the speckle pattern will be seen to change without translating, while as  $Z$  grows larger than  $|\rho|$ ,  $M$  becomes negative and increases rapidly — explaining the retrograde speckle movements observed earlier.<sup>(4)</sup>

### Conclusions

The following conclusions should be made for objective speckle sensitivity.

1. The use of a collimated illumination beam provides a measuring scheme for in-plane translation that is essentially independent of the distances between the source of illumination, the test surface and the sampling plane. However, this arrangement provides for no optical gain ( $M = 1$ ) and is, consequently, less sensitive.
2. The use of a noncollimated illumination beam provides for a measuring scheme whose sensitivity depends on both the radius of curvature of the beam at the surface and the distance to the objective speckle field sampling plane. This results from an optical gain relationship given by equation (1) describing a rotation of the objective speckle field about an "image" of the point source of illumination. This point of rotation lies at  $P'$  behind the test surface for divergent illumination ( $\rho$  positive), and at  $P''$  in front of the test surface for convergent illumination ( $\rho$  negative).
3. It may appear that this rotating objective speckle field model described by equation (1) suggests that either decreasing  $\rho$  or increasing  $Z$  provides simple means of achieving unlimited increases in  $M$  and sensitivity.

However, this study also shows that the need to know  $\rho$  with precision at all times (especially in the presence of out-of-plane motion) places a practical lower bound on  $\rho$ , while the loss of intensity with sampling distance imposes its own upper bound limitation in increasing  $Z$ .

4. If the point of origin,  $P$ , of a diverging illumination beam is positioned in the sampling plane so that  $\rho \equiv Z$ , the resulting  $M$  will equal 2 regardless of any out-of-plane movements of the surface. In other words, with the SMF and the MMB together in the same plane the sensitivity will be independent of  $Z$ , as it was with the collimated illumination, but at twice the magnification.

### Acknowledgments

The authors wish to acknowledge the support of the National Science Foundation under Grant No. MEA-8305597, and the contributions of Karl Leeb and the staff at American ACMI who provided the MMB used in these studies. They also wish to thank Karl Stetson of United Technologies Research Center and C. S. Vikram of Penn State University for their comments and suggestions.

### REFERENCES

1. Dudderar, T. D., Gilbert, J. A., Schultz, M. E. and Boehnlein, J. A., "The Application of Fiber Optics to Speckle Metrology," Proc. of the 1982 Joint Conference on Exp. Mechs., SESA/JSME, Oahu-Maui, Hawaii, 594-598, (May, 1982).
2. Gilbert, J. A., Dudderar, T. D. and Bennewitz, J. H., "The Application of Fiber Optics to Remote Speckle Metrology Using Incoherent Light," Optics and Lasers in Engrg., 3, 3, 183-196 (1982).
3. Dudderar, T. D. and Gilbert, J. A., "Fiber Optic Measurement of the Deformation Field on a Remote Surface Using Numerically Processed White Light Speckle," Applied Optics, 21, 19, 3520-3527 (1982).
4. Bennewitz, J. H., Dudderar, T. D., and Gilbert, J. A., "Objective Speckle Measurement," Proc. 1983 Spring (40th Anniversary) Conference of the SESA, Cleveland, Ohio, 113-118 (May 1983).
5. Dudderar, T. D., Gilbert, J. A., Boehnlein, A. J. and Schultz, M. E., "Application of Fiber Optics to Speckle Metrology — A Feasibility Study," Experimental Mechanics, 23, 3, 289-297 (1983).

TABLE I

	Z = 101.6 mm		
$\rho$ mm	S $\frac{\text{col}}{\text{mm}}$	M* $\frac{\text{mm}}{\text{mm}}$	$\frac{\rho + Z}{\rho}$
1.2 $\pm$ 0.50	3940	67.2	86.4
1.6 $\pm$ 0.50	3280	55.9	64.9
4.4 $\pm$ 0.50	1230	21.0	23.3
15.9 $\pm$ 0.50	396	6.8	7.4
25.4 $\pm$ 0.50	305	5.2	5.0
$\infty$ †	61	1.04	1.0

\*  $M = S/S_c$  where  $S_c = 58.6$  columns/mm

†  $\rho = \infty$  ... run with undiverged (collimated) laser beam.

TABLE II

	Z = 50.8 mm			Z = 203.2 mm			Z = 406.4 mm			Z = 812.8 mm		
$\rho$ mm	S $\frac{\text{col}}{\text{mm}}$	M <sup>■</sup> $\frac{\text{mm}}{\text{mm}}$	$\frac{\rho + Z}{\rho}$	S $\frac{\text{col}}{\text{mm}}$	M <sup>■</sup> $\frac{\text{mm}}{\text{mm}}$	$\frac{\rho + Z}{\rho}$	S $\frac{\text{col}}{\text{mm}}$	M <sup>■</sup> $\frac{\text{mm}}{\text{mm}}$	$\frac{\rho + Z}{\rho}$	S $\frac{\text{col}}{\text{mm}}$	M <sup>■</sup> $\frac{\text{mm}}{\text{mm}}$	$\frac{\rho + Z}{\rho}$
1.5 $\pm$ 0.50	1424	26.4	34.4	6216	115.3	134.7	10737	199.0	268.3	314195	584.0	535.7
3.1 $\pm$ 0.50	850	15.8	17.7	3108	57.6	67.7	5906	109.5	134.3	15748	292.0	267.5
6.1 $\pm$ 0.50	486	9.0	9.3	1712	31.7	34.3	3281	60.8	67.6	6218	115.3	134.2
12.2 $\pm$ 0.50	286	5.3	5.2	976	18.1	17.7	1817	33.7	34.3	3691	68.4	67.6
24.4 $\pm$ 0.50	165	3.1	3.1	479	8.9	9.3	909	16.8	17.7	1763	32.7	34.3
48.8 $\pm$ 0.50	110	2.0	2.0	273	5.1	5.2	482	8.9	9.3	945	17.5	17.7
76.2 $\pm$ 0.50	ND <sup>#</sup>	—	1.7	202	3.7	3.7	343	6.4	6.4	618	11.5	11.7
101.6 $\pm$ 0.50	ND	—	1.5	163	3.0	3.0	263	4.9	5.0	478	8.9	9.0

■  $M = S/S_c$  where  $S_c = 53.93$  columns/mm

# ND ... not determined because the objective speckle size was too small to be resolved by the system (less than 0.01 mm)



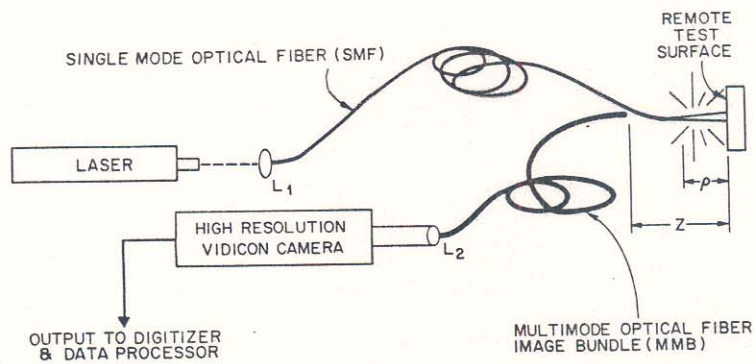


Figure 2 Log-log plot of the measured objective speckle magnification,  $M$ , versus the illumination beam radius of curvature,  $\rho$ , for five different observation distances.

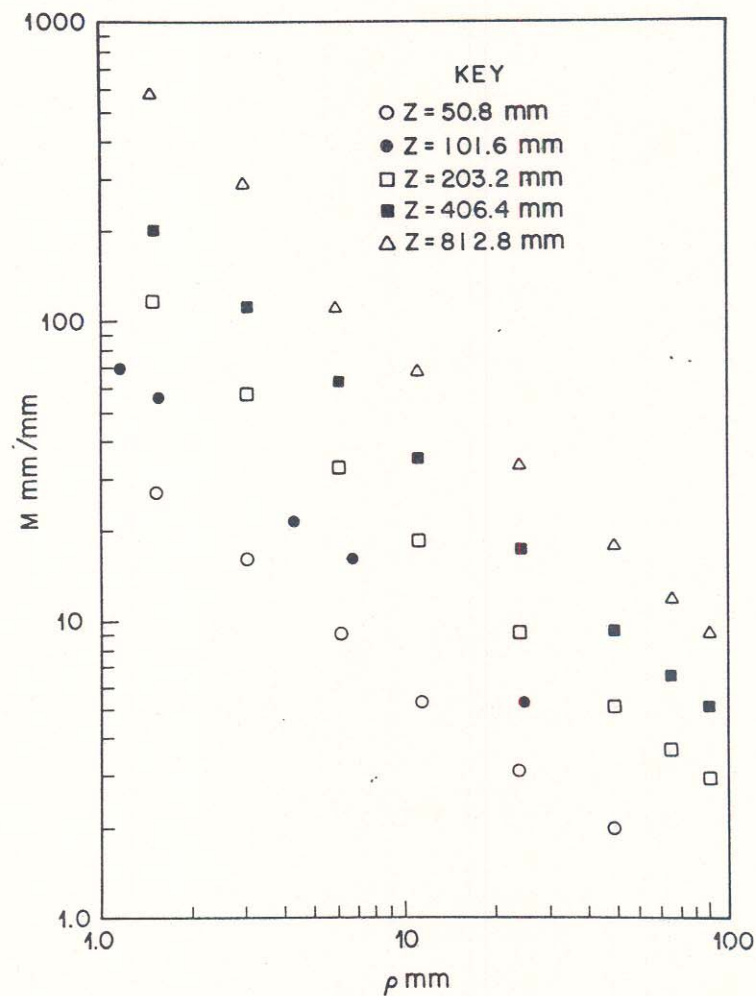


Figure 1 Schematic arrangement of the equipment used in studies of remote objective speckle metrology.

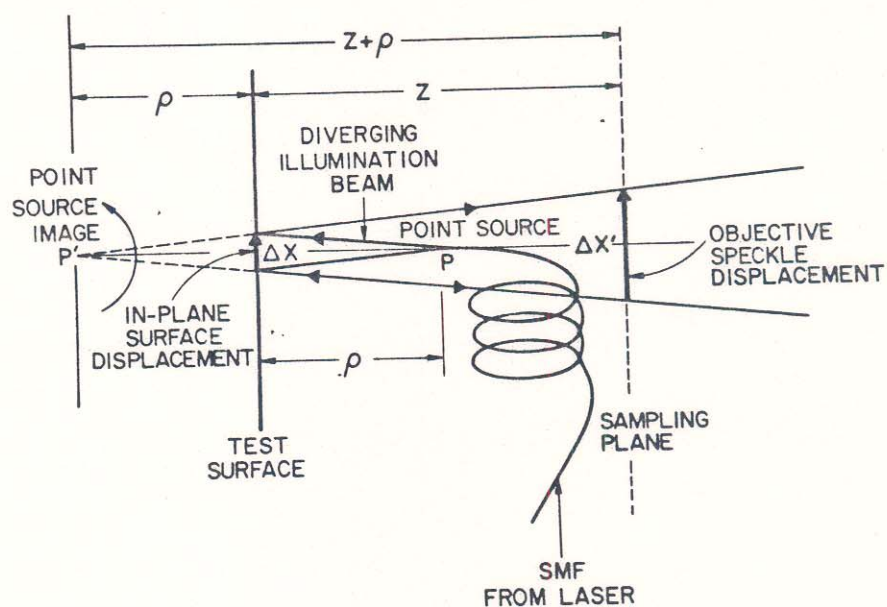


Figure 3 Diagrams of the object speckle pattern rotation and magnification in terms of the geometry for divergent illumination along the surface normal.

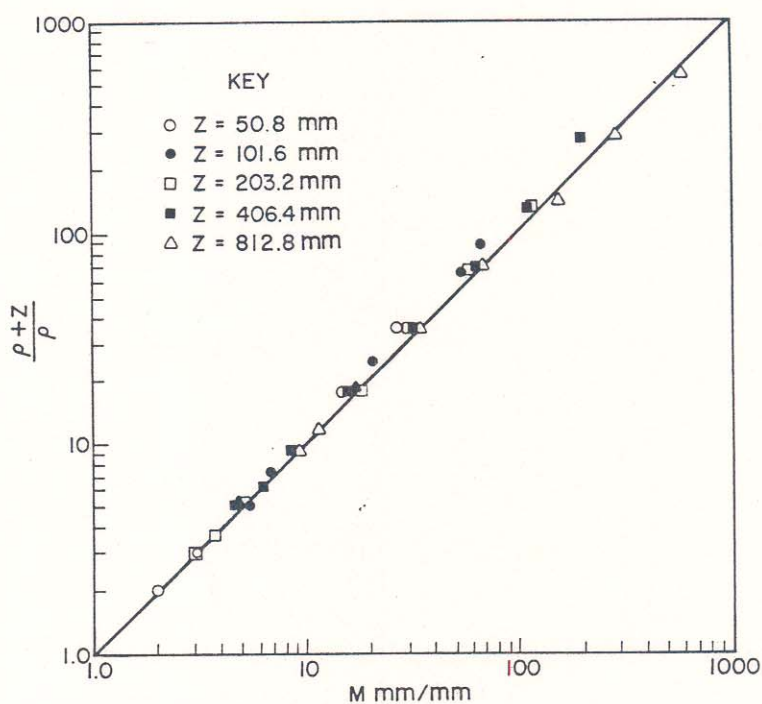


Figure 4 Log-log plot of  $(\rho + Z)/\rho$  versus the objective speckle magnification,  $M$ .